

Reduce Computational Complexity for Convolutional Layers by Skipping Zeros

Zhiyi Zhang, Pengfei Zhang, Zhuopin Xu, Qi Wang

Hefei Institutes of Physical Science

Chinese Academy of Sciences

Hefei, Anhui, China

gilgamesh@mail.ustc.edu.cn, pfzhang@aiofm.ac.cn, xuzp@iim.ac.cn, wangqi@ipp.ac.cn

Abstract—Deep neural networks rely on parallel processors for acceleration. To design operators for them, it requires not only good algorithm to reduce computational complexity, but also sufficient utilization of hardwares. Convolutional layers mainly contain 3 kinds of convolutional operators: convolution in forward propagation, deconvolution and dilated-convolution in backward propagation. When executing these operators, 0s are always added to tensors, causing redundant calculations. This paper presents the *C-K-S* algorithm (*ConvV2*, *KS-deconv*, *Sk-dilated*), which skips these 0s in two ways: trim the filters to exclude padded 0s; transform sparse tensors to dense tensors, to avoid inserted 0s in deconvolution and dilated-convolution. In contrast to regular convolution, deconvolution is hard to accelerate on GPUs due to its complicity. This paper provides high-performance GPU implementations of *C-K-S*, and verifies their effectiveness with comparison to PyTorch (cuDNN). According to the experiments, *C-K-S* has advantages over PyTorch in certain cases, especially in deconvolution on small feature-maps. Further optimizations of *C-K-S* can be made by targeting specific GPU architectures.

Keywords—convolutional neural networks, deconvolution, dilated-convolution, graphic processing units.

I. INTRODUCTION

Convolutional layers (conv-layers) are widely used in deep neural networks (DNNs) [2]–[6], with advantages of parameter sharing, sparse interactions and equivariant representations [1]. Conv-layers primarily include 3 kinds of convolutional operators: convolution, deconvolution (transposed convolution) and dilated-convolution. These 3 kinds of operators take the most resource in training convolutional neural networks (CNNs), so it's always a key issue to optimize them.

Convolution and deconvolution are a pair of inverse operators. Generally, convolution is for down-sampling to reduce feature-size, while deconvolution performs up-sampling to expend features. For conv-layers, convolution generates output-features in forward propagation, whereas deconvolution finds the gradients of input-features in backward propagation [16]. The opposite is true for deconvolutional layers. Besides, dilated-convolution is used to find the gradients of filters.

In propagations of Conv-Layers, zero-elements (0s) are inevitably added to tensors, in order to generate tensors with expected-size, or construct sparse tensors to find gradients. Such 0s cause redundant calculations (0-calculations), so the

computational complexity can be reduced by skipping them.

The efficient implementations [7]–[15] of conv-layers are mainly based on parallel processors including GPU and FPGA, due to their superiority in accelerating intensive operations such as convolution and matrix-multiply. To design operators for DNNs, algorithms with low complexity, and the adaptability to hardwares are both important.

This paper presents the *C-K-S* algorithm, which not only skip 0-calculations to lower the complexity of conv-layers, but also has efficient GPU implementations. *C-K-S* consists of *ConvV2*, *KS-deconv* and *Sk-dilated*, and these 3 parts respectively orient to convolution, deconvolution and dilated-convolution. For Dragon-Alpha [15][21], *C-K-S* is an indispensable factor to achieve high-performance. In relevant experiments, Dragon-Alpha spent less time and memory than PyTorch [13] to train some typical DNNs [2]–[5] on Cifar10 [25]. Therefore, this paper is also a summary of convolution techniques in Dragon-Alpha.

This article uses ‘is’ for ‘features’ and ‘filters’ to see them as a whole. To more simply express time-complexity, n refers the size of data. The relevant parameter notations for 2D conv-layers are listed in Table I.

TABLE I. PARAMETER NOTATIONS FOR 2D CONV-LAYERS

Notation	Explanation
*	Scalar-multiply or Convolution
\times	Cartesian-product or matrix-multiply
\odot	Element-wise multiply
$\langle \cdot \rangle$	Matrix or Vector
in-range-of	Return true if an index is within the range of a tensor, otherwise return false
$X \setminus Y \setminus W$	input-features \ output-features \ filters
$X_{n, ih, iw, ic}$	An indexed element in X
$Y_{n, oh, ow, oc}$	An indexed element in Y
$W_{oc, fh, fw, ic}$	An indexed element in W
$I_H \setminus I_W$	Height \ Width of X
$O_H \setminus O_W$	Height \ Width of Y
$F_H \setminus F_W$	Height \ Width of W
$N \setminus I_C \setminus O_C$	Batchsize \ Input-channels \ Output-channels
$sh \setminus sw$	Stride on height \ width axis of convolution in forward propagation
$ph \setminus pw$	Padding on height \ width axis of convolution in forward propagation

II. MOTIVATION

In conv-layers, to generate output-features with expected size, certain 0s may be padded on the boundary of the input-features X . In many DNNs, due to down-sampling, the feature-maps become smaller with going deeper. In shallow layers, the proportion of the padded 0s in X is small. But it

This research was supported by National Natural Science Foundation of China (No. 32070399); Anhui Science and Technology Major Project (No. 202103a06020014), the Chinese Academy of Sciences-Henan Province Achievement transfer and Transformation Project (No. 20222208); Hefei Science and Technology Project (No. 2021GJ065).

could be large enough in deeper layers, resulting in a non-negligible number of 0-calculations. Fig. 1 gives an example, in the case of 2D-convolution with padding-1 stride-1 and (3×3) filters. The red curve represents the proportion of padded 0s in X , while the blue indicates the proportion of 0-calculations in the total amount. Such 2 proportions become bigger, as the size of feature-maps ($F \times F$) decreases.

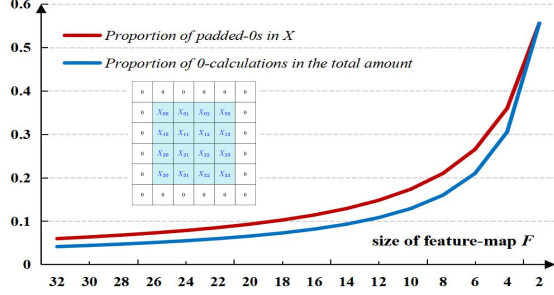


Fig. 1. padding causes more 0-calculations on smaller feature-maps.

When stride of convolution is greater than 1, (stride - 1) 0s will be inserted between adjacent elements of ∇Y , in order to find ∇X and ∇W through deconvolution and dilated-convolution. The inserted 0s account for a big proportion in ∇Y making it a sparse tensor, and leading to massive 0-calculations, especially when stride is big. As shown in Fig. 2, only calculations between the colored elements are necessary, and the rest are otiose.

To avoid 0-calculations, *ConvV2* trims the filters to exclude the padded 0s, while *KS-deconv* and *SK-dilated* transform ∇Y back to dense tensor by filter-reconstruction and leaping-element-access to avoid the inserted 0s.

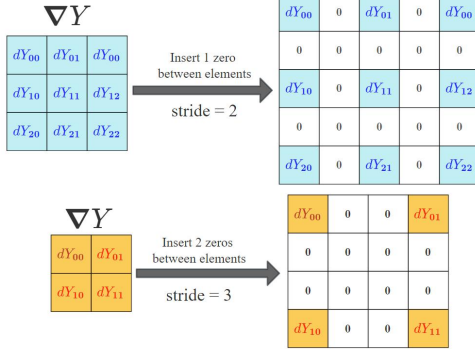


Fig. 2. Insert (stride - 1) 0s between adjacent elements of ∇Y .

GPU [22][23] is good at intensive computation due to its SIMD nature, which is also the reason for its weakness in executing conditional statements. GPU memory is high bandwidth but low capacity, and is therefore a scarce resource. When directly handling these added 0s, GPUs need either auxiliary memory or conditional statements, that hurts the spatial or temporal efficiency. To maximize the hardware performance, the GPU implementations of *C-K-S* are mainly dense kernel-functions, with minimized auxiliary memory and conditional statements.

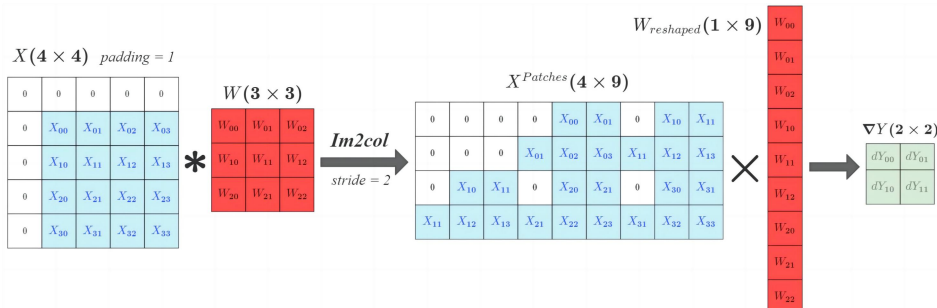


Fig. 3. Through *im2col*, the 2D-convolution $X * W$ can be transformed to matrix-multiply $X^{\text{Patches}} \times W^{\text{reshaped}}$.

III. BACKGROUND

A. Approaches to Implement 2D-Convolution on GPUs

The approach of A. Krizhevsky [8] is to compute the convolution directly. It's very efficiency in some cases, but may be poor in the others, and requires many specialized implementations for the corner cases of convolution.

FFT convolution has much lower time-complexity in theory than dense convolution, but has many drawbacks. It needs much temporary memory to pad filters the same size as input-feature-maps, and has lower performance in the case of small-filter or big-stride. Besides, FFT is a recursive algorithm with conditional statements, and its computation is not as intensive as dense convolution, so it gets less acceleration on GPUs.

Caffe [12] lowers 2D-convolution to matrix-multiply by *im2col* (Fig. 3). This approach is efficient and robust based on well-optimized matrix-multiply libraries, but it needs auxiliary memory to store the unfolded tensors. CuDNN [9] optimized this approach, by implicitly integrating *im2col* to General-Matrix-Multiply (GEMM) operators, to improve the speed without auxiliary memory.

The *direct* [8] and *implicit-GEMM* [9] approaches are referred to implement *C-K-S* on GPUs. Since deconvolution and dilated-convolution are special kinds of convolution, it's feasible to implement them in a similar way to convolution.

B. Related Works

For deconvolution, the distribution of inserted 0s is different in each patch of ∇Y , leading to its complicity. The main work of accelerating deconvolution is usually to avoid 0-calculations, and simplify the control on hardwares.

Orosa *et. al.* [17] devise a compile-time computation scheduling for deconvolution, to remove 0-calculations with minimal overhead. Cutlass [10] provides implementations of *strided_dgrad*, which skips 0-calculations by thread indices, but may not be universally applicable due to its specificity for CUDA's architecture. J. Chang *et. al.* [18] present the TDC method with FPGA implementations, to transform sparse-deconvolution to dense-convolution. K. Chang *et. al.* [19] and A. M. Vadakkevedu *et.al.* [20] decompose the convolutional kernel to multi smaller kernels, to exclude 0-calculations. Their implementations are respectively based on TSMC-40nm-CMOS-technology and TensorFlow [11].

The kernel-decomposition ideas [18]-[20] are somewhat close to *KS-deconv*, but there exits some differences between them. *KS-deconv* has lower time-complexity than TDC [18], because it decomposes smaller kernels. In the work of [19] and [20], their decomposition results are similar to *KS-deconv*'s in several specific cases, but they don't provide explicit math-formulas to make general comparisons. In addition, this work implemented *KS-deconv* on different architectures, and combined it with *ConvV2* to attain higher performance.

IV. ALGORITHM AND IMPLEMENTATION

The 2D-convolution of DNNs is with channels and batches, so the input-feature $\mathbf{X} \in \mathbf{R}^{N \times I_H \times I_W \times I_C}$, output-features $\mathbf{Y} \in \mathbf{R}^{N \times O_H \times O_W \times O_C}$ and filters $\mathbf{W} \in \mathbf{R}^{O_C \times F_H \times F_W \times I_C}$ are all 4D tensors. For 2D conv-layers, its forward propagation is represented as (1), while its backward propagation is represented as (2) and (3).

$$\mathbf{Y} = \text{conv}_{2D}(\mathbf{X}, \mathbf{W}) \quad (1)$$

$$\nabla \mathbf{X} = \text{deconv}_{2D}(\nabla \mathbf{Y}, \mathbf{W}^{\text{rot}180}) \quad (2)$$

$$\nabla \mathbf{W} = \text{dilated_conv}_{2D}(\mathbf{X}, \nabla \mathbf{Y}) \quad (3)$$

ConvV2 is described from the perspective of forward propagation, while *KS-deconv* and *Sk-dilated* are in a view of backward propagation. All pseudo code of algorithms are concentrated in Appendix.

A. ConvV2: Convolution with Trimmed Filters

To perform 2D-convolution, \mathbf{W} is used as a sliding window to generate patches of \mathbf{X} with padded 0s. In a specific patch, the padded 0s only appears at the boundary, while the other meaningful elements are in the center to form a rectangle. The start-position (fh_s, fw_s) of these meaningful elements is in the top-left corner, and the end-position ($fh_e - 1, fw_e - 1$) is in the down-right corner.

ConvV2 trims the height and width of \mathbf{W} to ($fh_e - fh_s$) and ($fw_e - fw_s$), in order to only cover the meaningful part from the start-position to the end, so that all padded 0s are not involved in calculation, thus reducing the time-complexity. As shown in Fig. 4, within the current sliding window, \mathbf{W} is trimmed from (3×3) to (2×2). The time-complexity of *ConvV2* is 50, that's smaller than the 72 of normal convolution (Fig. 3). The pseudo code of *ConvV2* is in Algorithm. 1.

In the practical implementations, *padding* is achieved by conditional-statements: when fetching an element with a specific index, return its value if the index is in range, but 0 if not. Such logical *padding* sacrifices a little speed, but saves lots of memory. Because *ConvV2* excludes all padded 0s, there is no conditional statements for logical *padding*, which improves the efficiency.

When the size of \mathbf{X} is large enough, to improve memory bandwidth, the dimension order of \mathbf{W} will be changed from ($O_C \times F_H \times F_W \times I_C$) to ($F_H \times F_W \times I_C \times O_C$) with $\theta(n)$ complexity, that brings about 6% increase on speed.

B. KS-deconv: Kernel-Split Deconvolution

The *KS-deconv* is used for deconvolution with stride greater than 1. Otherwise, the direct approach is simpler and faster, due to the density of $\nabla \mathbf{Y}$. *KS-deconv* consists of 3 stages, and its pseudo code is in Algorithm 2.

Stage1 kernel-split (Fig. 5): rotate \mathbf{W} 180 degrees, then split \mathbf{W} to construct ($sh * sw$) smaller kernels. The shape of the (y, x)_{th} smaller kernel $\mathbf{C}_{y,x}$ is ($O_C \times \lfloor \frac{F_H - y}{sh} \rfloor \times \lfloor \frac{F_W - x}{sw} \rfloor \times I_C$).

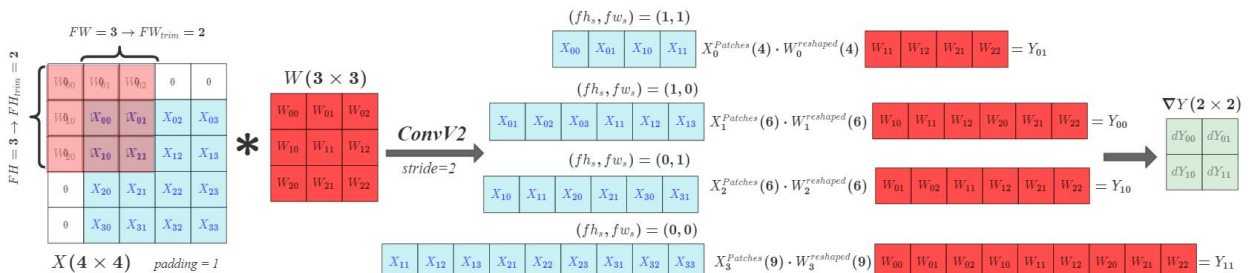


Fig. 4. *ConvV2* trims filters to exclude all padded 0s.

Finally, concat all smaller kernels to a 6D tensor $\mathbf{C} \in \mathbf{R}^{sh \times sw \times O_C \times \lfloor \frac{F_H}{sh} \rfloor \times \lfloor \frac{F_W}{sw} \rfloor \times I_C}$ with continuous mem-addresses.

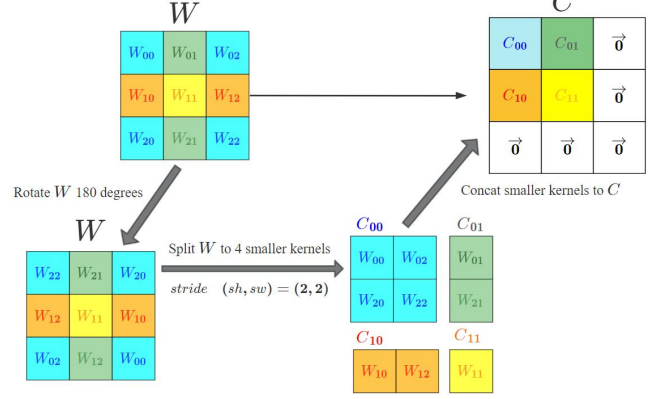


Fig. 5. *KS-deconv* Stage1: rotate \mathbf{W} 180 degrees. Split $\mathbf{W}(3 \times 3)$ to 4 smaller kernels $\mathbf{C}_{00}(2 \times 2)$, $\mathbf{C}_{01}(2 \times 1)$, $\mathbf{C}_{10}(2 \times 1)$ and $\mathbf{C}_{11}(1 \times 1)$. Concat \mathbf{C}_{00} , \mathbf{C}_{01} , \mathbf{C}_{10} and \mathbf{C}_{11} to $\mathbf{C}(2 \times 2 \times 2 \times 2)$, which has continuous memory addresses.

Stage2 stride-1-convolution (Fig. 6): perform stride-1 convolutions on $\nabla \mathbf{Y}$ with each $\mathbf{C}_{y,x}$ to generate ($sh * sw$) outputs. The (y, x)_{th} convolution is specifically with padding $\langle oph_{y,x}, opw_{y,x} \rangle$, and a start-position (ih_s, iw_s) mapping to the top-left corner of an area in $\nabla \mathbf{X}$. Based on these start-positions, $\nabla \mathbf{Y}$ are trimmed to avoid needless calculations.

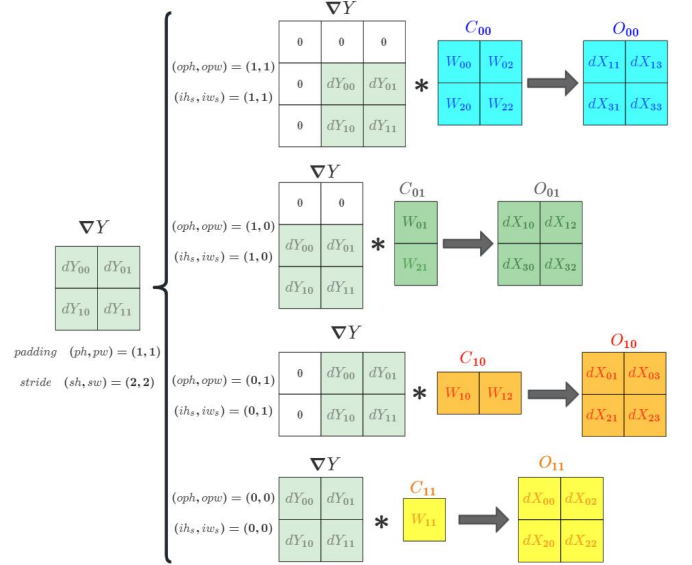


Fig. 6. *KS-deconv* Stage2: perform stride-1 convolution on $\nabla \mathbf{Y}$ with \mathbf{C}_{00} , \mathbf{C}_{01} , \mathbf{C}_{10} and \mathbf{C}_{11} respectively to generate \mathbf{O}_{00} , \mathbf{O}_{01} , \mathbf{O}_{10} and \mathbf{O}_{11} .

Stage3 grad-composition (Fig. 7): compose all ($sh * sw$) outputs to get $\nabla \mathbf{X}$. To remove unnecessary calculations, $\langle ih_s, iw_s \rangle$ is adjusted to non-negative. When $\langle I_H, I_W \rangle$ is an integral multiple of $\langle sh, sw \rangle$, there is no need to check whether $\langle ih, iw \rangle$ is within the range of $\nabla \mathbf{X}$, and the efficiency will be improved due to reduction of conditional statements.

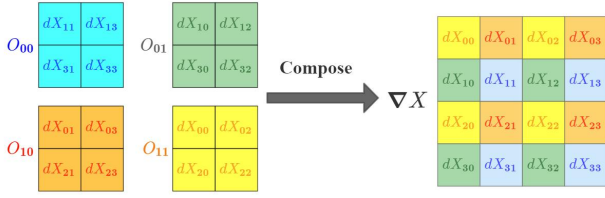


Fig. 7. *KS-deconv* Stage3: compose O_{00} , O_{01} , O_{10} and O_{11} to get ∇X .

The time-complexity of *KS-deconv* is $\theta(n^3)$, and that of the direct method is $\theta(sh * sw * n^3)$, which is $(sh * sw)$ times of the first. As the stride increases, the gap between the two grows rapidly.

Stage2 and Stage3 are merged, so that Stage3 can directly use the outputs of Stage2 in registers to reduce overhead. Stage1 needs $(sh * sw * O_C * \lceil \frac{F_H}{sh} \rceil * \lceil \frac{F_W}{sw} \rceil * I_C)$ auxiliary memory to store C . In most cases, C takes much less memory than ∇Y and ∇X , and Stage1 has fairly smaller time-complexity than Stage2. Therefore, the cost of Stage1 is acceptable, and can be ignored when batchsize and feature-size are large enough.

This work made an contrast implementation, where Stage1 is achieved by index-conversion rather than auxiliary memory, and all 3 stages are merged to a whole. But it's slower, mainly because of the overhead caused by discontinuous memory-access and index-calculation.

C. *Sk-dilated*: Skip 0s in Dilated-Convolution

In dilated-convolution, ∇Y performs as filters, so the distribution of inserted 0s is fixed for all patches of X . Suppose $(sh - 1)$ and $(sw - 1)$ 0s are respectively inserted between adjacent elements of ∇Y along the height and width axes, (n, oh_p, ow_p, oc) is the index of a specific element in ∇Y . Such element is not an inserted 0 if $\langle oh_p, ow_p \rangle$ is an integral multiple of $\langle sh, sw \rangle$, otherwise it is.

Follow this rule, *Sk-dilated* doesn't insert 0s to ∇Y , but fetches elements in leaping steps $\langle sh, sw \rangle$ to generate patches. As shown in Fig. 8, within the current sliding window, elements are fetched according to this 2D-index sequence: $(0, 0) \rightarrow (0, 2) \rightarrow (2, 0) \rightarrow (2, 2)$. Algorithm. 3 presents the pseudo code of *Sk-dilated*.

The time-complexity of *Sk-dilated* is $\theta(n^3)$, and that of the direct approach is $\theta(sh * sw * n^3)$ which is $(sh * sw)$ times of the first. With the increase of stride, the gap between the two rapidly grows.

Through *im2col*, the *Sk-dilated-convolution* between X and ∇Y , can be lowered to a matrix-multiply between $A \in \mathbb{R}^{G_N \times G_K}$ and $B \in \mathbb{R}^{G_K \times G_M}$, where $G_N = O_C$, $G_M = F_H * F_W * I_C$ and $G_K = N * O_H * O_W$. But G_N and G_M don't increase with feature size, if the number of thread-blocks is only determined by them, the parallelism of GPU may be insufficient. The 'map-reduce' model is referred to solve this problem: split A

and B to G_Z segments along G_K axis, then compute these segments in parallel, finally sum up all G_Z local results to get the global result. Since the computations on segments take the most of time-complexity, the parallelism becomes about G_Z times of the original.

The following method is used to decide G_Z . In conv-layers, a dilated-convolution γ corresponds to a convolution α and a deconvolution β . Without map-reduce, their number of thread-blocks are N_α , N_β and N_γ . Since N_α and N_β increase with feature-size, G_Z can be positive related to $(N_\alpha + N_\beta) / N_\gamma$. It also needs a lower and upper bound to restrict G_Z . The upper bound can be decided by the number of SMs in GPU.

D. Combination: *KS-deconv-V2* and *Sk-dilated-V2*

The *V2* versions of *KS-deconv* and *Sk-dilated* combines the filter-trimming of *ConvV2*. So they perform better especially on small feature-maps, due to less complexity and conditional-statements. *KS-deconv-V2* has 3 stages, and only the second stage is different from that of *KS-deconv*, where the stride-1 convolutions are achieved by *ConvV2*. The same as *Sk-dilated*, *Sk-dilated-V2* also needs map-reduce to raise parallelism. Their pseudo code are in Algorithm 2B and 3B. Fig. 9 and 10 present how they work by examples.

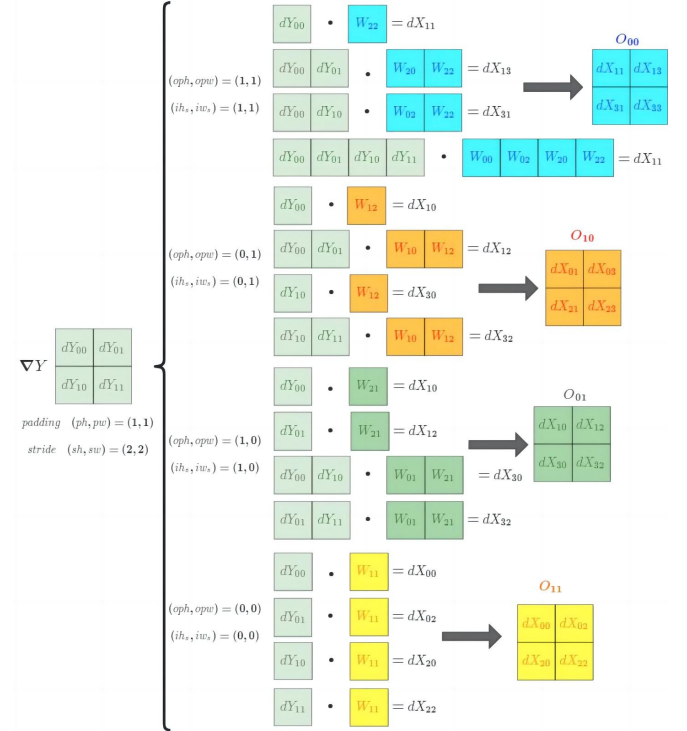


Fig. 9. *KS-deconv-V2* Stage2 (Fig. 5 for Stage1, Fig. 7 for Stage3): the stride-1 convolutions are achieved by *ConvV2*. The time-complexity is 50, less than the 72 of *KS-deconv* Stage2 (Fig. 6).

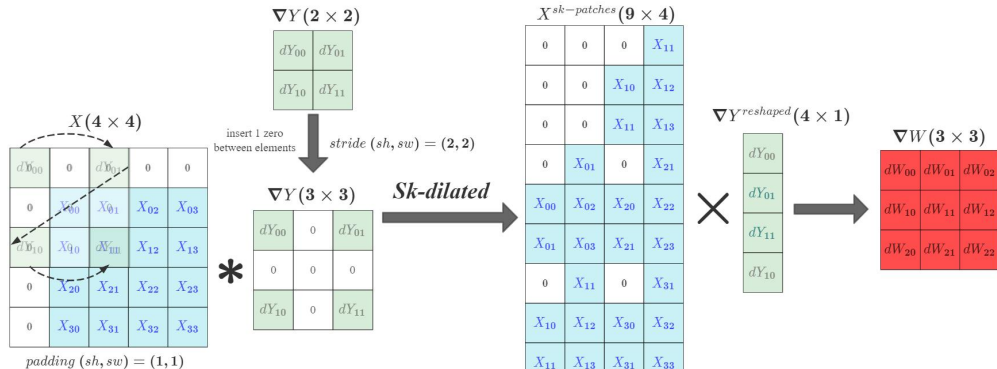


Fig. 8. *Sk-dilated* fetches elements in leaping-steps to generate patches.

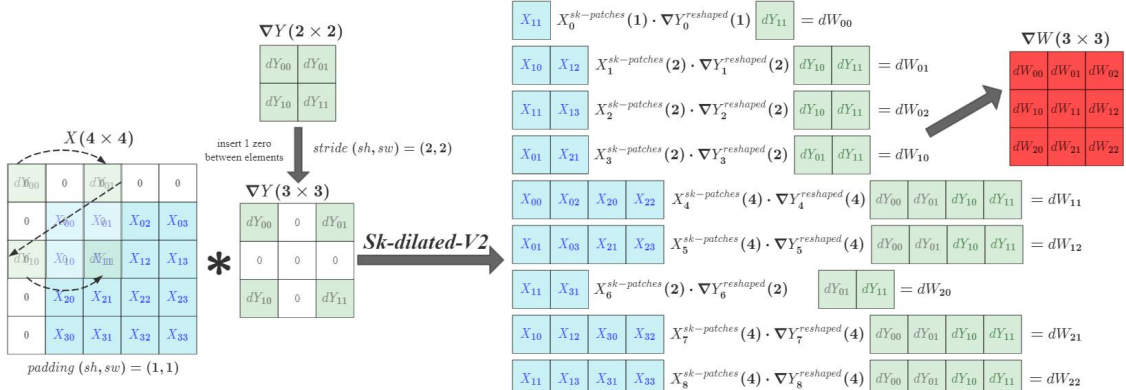


Fig. 10. *Sk-dilated-V2*: padded 0s are excluded. The time-complexity is 50, less than the 72 of *Sk-dilated* (Fig. 8).

E. GPU Optimizations

More than 100 kernel-functions have been implemented for *C-K-S-V2* (*C-K-S* with *KS-deconv-V2* and *Sk-dilated-V2*). Some of them are general solutions to assure performance, while some are specialized to have higher performance in specific situations. For convenience, they are aggregated to make a higher-level encapsulation [15].

GPU executes integer division and remainder operations much slower than floating-point operations, so their usage should be minimized. In some cases, they are replaced by cheap bitwise-operations. For codes with strict requirements for high-performance, the results of these integer operations will be pre-calculated, then stored in constant-memory to maximize the broadcast, and will be retrieved by kernel-functions during calculating.

GPU is not good at handling conditional statements for its SIMD nature. Therefore, some conditional statements are replaced by equivalent tables and expressions. Besides, some fixed-loops are unrolled manually or by compilers, to remove the conditional statements which control the loops.

The last dimension of tensors are implicitly padded to $4x$, and some memory operations are merged through vector-types, in order to improve the bandwidth by using 128bit as the minimum unit for memory access.

For dense kernel-functions, *im2col*, *reshape*, *transpose*, *padding*, etc operators are integrated to them, and achieved by index-conversion with no auxiliary memory. Double-buffered shared-memory is used to hasten data loading. Some statements are reordered to reduce the consumption of registers. Each thread executes a big batch of instructions per round to hide memory access, for example: in the heaviest kernel-functions of *ConvV2*, each thread execute $(8 \times 8 \times 16)$ multiply-add operations, after each round of reading data from global-memory.

V. EXPERIMENTS

In this work, the GPU implementations of *C-K-S-V2* are improved from cu32 of Dragon-Alpha [15][21]. This section discusses their performance and the variation tendencies. PyTorch (1.12.1) [13] is used as a baseline for comparison, since its underlying GPU library cuDNN [9] has been extremely optimized. *ConvV2* is evaluated from the perspective of forward propagation, while *KS-deconv (-V2)* and *Sk-dilated (-V2)* are in a view of backward propagation. To know the overall performance of *C-K-S* in DNNs, please refer the experimental datas of Dragon-Alpha [15].

A. Methods

For each member of *C-K-S-V2*, 2 test-sets with different

filter-size are provided, and each test-set contains 8 test-cases. From the 1st to the 8th test-case, the feature-size goes smaller, but channels and batchsize become bigger. The stride or dilation is 2 to introduce sparse tensor.

The operators were tested on RTX 3060ti GPU with CUDA 11.5 in *float32* data-type. The operations of *C-K-S* and PyTorch are logically equivalent, with the same time-complexity. All calculations were performed on GPU, and there was no data transmission between GPU and CPU. At the same time, only 1 operator was executed to grasp all GPU resource, while the interference from other programs was minimized. The size of input data is large enough to ensure parallelism. To maximize PyTorch's speed, it pre-allocated enough memory before loops of executing a specific convolutional operator; and it didn't do any *rotate* or *transpose* operations to change arrangement of tensors, but just executed convolutional operators.

Each operator was executed 1000 times in succession for each of their test-cases, and *cudaDeviceSynchronize()* was called to ensure completion of each execution. The total execution time was averaged, to find the speed of floating-point operation (time-complexity / time), where the unit is GFlop/s (10^9 *float32* operations per second). Formulas for time-complexity of convolutional operators are in Table II.

TABLE II. FORMULAS FOR TIME-COMPLEXITY

Formula	Explanation
$T_{Conv} = 2 * (O_C * N * O_H * O_W * F_H * F_W * I_C)$	Time-complexity of 2D-Convolution.
$T_{Deconv} = 2 * (I_C * N * I_H * I_W * F_H * F_W * O_C)$	Time-complexity of 2D-Deconvolution.
$T_{Dilated} = 2 * (O_C * F_H * F_W * I_C * O_H^p * O_W^p)$	Time-complexity of 2D-Dilated-Convolution.
$O_H^p = O_H + (O_H - 1) * (sh - 1)$	The height of ∇Y with inserted $(sh - 1)$ 0s.
$O_W^p = O_W + (O_W - 1) * (sw - 1)$	The width of ∇Y with inserted $(sw - 1)$ 0s.

B. Results

Line-charts are used to demonstrate the variation of speed under different tensor shapes. Fig. 11-12 show the results of convolution, where the “*” means excluding the time of changing the dimension order of W . Fig. 13-14 present the results of deconvolution, and Fig. 15-16 list the results of dilated-convolution.

C. Discussions

In deconvolution, *KS-deconv* has better performance in all 16 cases than PyTorch. In convolution and dilated-convolution, PyTorch is faster in the middle cases, while the results are opposite in the other cases. In most CNNs, the

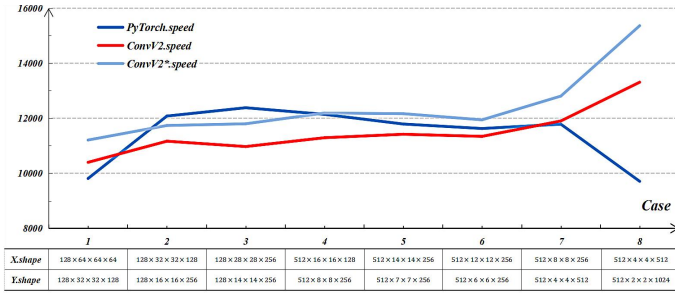


Fig. 11. Convolution: $\langle F_H F_W \rangle = \vec{3}, padding = 1$.



Fig. 12. Convolution: $\langle F_H F_W \rangle = \vec{5}, padding = 2$.

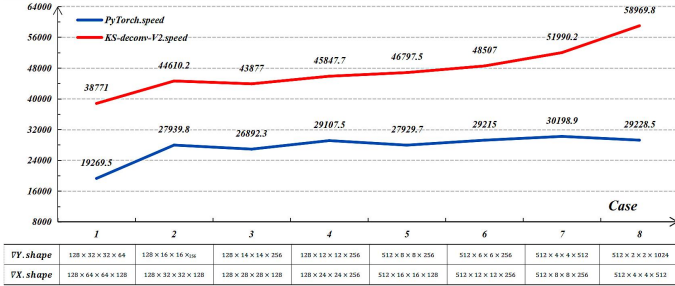


Fig. 13. Deconvolution: $\langle F_H F_W \rangle = \vec{3}, padding = 1$.

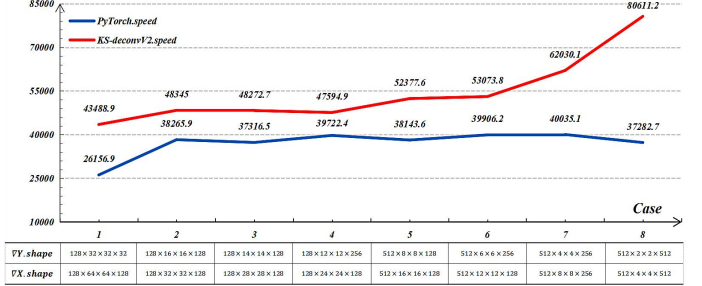


Fig. 14. Deconvolution: $\langle F_H F_W \rangle = \vec{5}, padding = 2$.

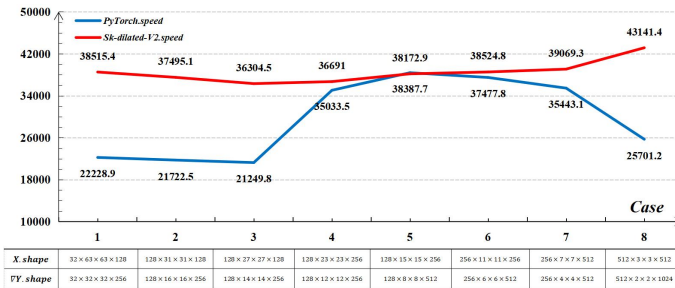


Fig. 15. Dilated-Convolution: $\langle F_H F_W \rangle = \vec{3}, padding = 1$.

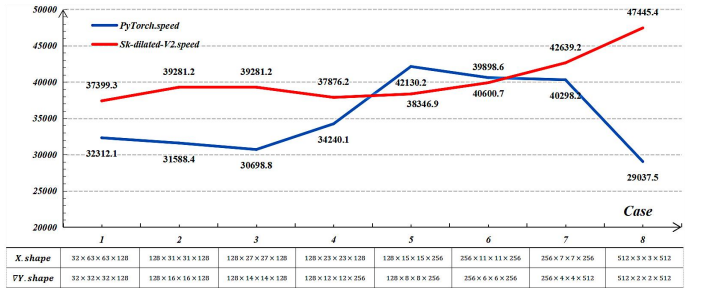


Fig. 16. Dilated-Convolution: $\langle F_H F_W \rangle = \vec{5}, padding = 2$.

deeper layers with bigger channels and smaller feature-size, usually cause the majority of time-complexity. Therefore, cuDNN made full optimizations for them, to be more efficient than this work's implementations. But due to the filter-trimming, the speed of *ConvV2* and *Sk-dilated-V2* finally exceeds that of PyTorch. In conclusion, the above comparison verifies the effectiveness of this work's GPU implementations of *C-K-S-V2*.

Benefiting from filter-trimming, in general, *C-K-S-V2* is faster with smaller feature-size and bigger padding, since more padded 0s are excluded. Due to down-sampling, in all test-cases, the size of output feature-maps is smaller than that of input feature-maps, so the filter-trimming plays more roles in deconvolution, leading to a higher speed.

In deconvolution and dilated-convolution, ∇Y expands nearly 4 times because of the inserted 0s. But these 0s are skipped through *KS-deconv* and *Sk-dilated*, resulting in the following two gains: first, the actual time-complexity is only about 25% of that in theory; second, there is no sparse tensor involved in calculation, therefore, the design pattern of *ConvV2*'s kernel-functions for dense computing, can be naturally migrated to those of *KS-deconv* and *Sk-dilated*, so that they can efficiently utilize the GPU to a similar extent. That's why the speed of *KS-deconv* and *Sk-dilated* is close to 4 times of *ConvV2*'s.

But it's difficult to exceed such '4 times', due to their complicity compared to *ConvV2*. *KS-deconv* needs additional resources to reconstruct filters, and more registers for intermediate variables, which lowers the parallelism of dense kernels because of less active threads. The *Sk-dilated*

relies on map-reduce to have sufficient parallelism, that inevitably causes certain expenses. In addition, its memory access is less continuous with larger spans, that hurts the hit-radio of L2-cache.

The heaviest kernel functions of *C-K-S-V2* refers the *implicit-GEMM* [9] approach, and are selected to handle large-scale data, so their performance remains stable in all test cases. When handling large-scale data, the speed of *ConvV2* can improve by 5% to 10%, without the time of dimension-reordering of W , and such reordering can be avoided with better tensor arrangement, or be hidden in the parallel execution of multi operators. When using *ConvV2* or *KS-deconv* to perform one-way propagation, it's able to reconstruct the filters before loops of convolutional operators, as it can further reduce the time of computation.

VI. CONCLUSION

This paper discusses the motivation, background, algorithms as well as the implementations of *C-K-S*, and verifies its effectiveness by experiments with comparison to PyTorch. *C-K-S* skips 0-calculations in two ways: exclude the padded 0s by filter-trimming, and transform ∇Y back to dense tensor to avoid the inserted 0s. *C-K-S* reduces the computational complexity in theory, and gets on well with GPUS to have high-performance. As a result, it has the potential to break the limit of devices' compute capability.

Certain optimizations for GPUs were made in this work, but not full optimization oriented to the Ampere architecture [24] to extremely utilize the hardware. The bank-conflict on shared-memory hasn't been thoroughly solved, that lowers the performance. All GPU programming is by C++ without

integrated ptx-codes, and the executable files are directly generated by the compiler with no fine-tuning on sass-codes. For elements fetching of convolutional operators, the memory bandwidth was improved, but the overlaps between patches haven't been fully used. Further enhancements can be made according to the aforementioned defects.

REFERENCES

- [1] I. Goodfellow, T. Bengio and A. Courville, "Deep Learning," [Online]. Available: <https://www.deeplearningbook.org>.
- [2] A. Krizhevsky, I. Sutskever and G. E. Hinton, "Imagenet classification with deep convolutional neural networks," in *Proc. NIPS*, 2012, pp. 1097-1105.
- [3] K. Simonyan and A. Zisserman, "Very Deep Convolutional Networks for Large-Scale Image Recognition," [Online]. Available: <https://arxiv.org/abs/1409.1556>.
- [4] C. Szegedy, W. Liu, Y. Jia, P. Sermanet, S. Reed, D. Anguelov, *et al.*, "Going deeper with convolutions," [Online]. Available: <https://arxiv.org/abs/1409.4842v1>
- [5] K. He, X. Zhang, S. Ren, and J. Sunn, "Deep residual learning for image recognition," in *Proc. CVPR*, Jun. 2016, pp. 770-778.
- [6] Z. Liu, H. Mao, C. Feichtenhofer, C. Feichtenhofer, T. Darrell and S. Xie, "ConvNext: A ConvNet for 2020s," [Online]. Available: <https://arxiv.org/abs/2201.03545>.
- [7] Travis Oliphant, "NumPy: A guide to NumPy," [Online]. Available: <https://numpy.org>.
- [8] A. Krizhevsky, "cuda-convnet2," [Online]. Available: <https://code.google.com/p/cuda-convnet2>.
- [9] S. Chetlur, C. Woolley, P. Vandermerse, J. Cohen and J. Tran, "cuDNN Efficient Primitives for Deep Learning," [Online]. Available: <https://arxiv.org/abs/1410.0759v3>.
- [10] A. Kerr, H. Wu, M. Gupta, D. Blasig, P. Ramini, D. Merrill, *et al.*, "CUTLASS," [Online]. Available: <https://github.com/NVIDIA/cutlass>.
- [11] M. Abadi, A. Agarwal, P. Barham, E. Brevdo, Z. Chen, C. Citro, *et al.*, "TensorFlow: Large-scale machine Learning on heterogeneous system," [Online]. Available: <https://arxiv.org/abs/1603.04467v2>.
- [12] Y. Jia, E. Shelhamer, J. Donahue, S. Karayev, J. Long, R. Girshick, *et al.*, "caffe: Convolutional architecture for fast feature embedding," [Online]. Available: <https://arxiv.org/abs/1408.509>.
- [13] A. Paszke, S. Gross, F. Massa, A. Lerer, J. Bradbury, G. Chanan, *et al.*, "PyTorch: An Imperative Style, High-Performance Deep Learning Library," [Online]. Available: <https://arxiv.org/abs/1912.01703v1>.
- [14] Tencent, "NCNN," [Online]. Available: <https://github.com/Tencent/ncnn>.
- [15] Z. Zhang, P. Zhang and Q. Wang, "Dragon-Alpha&cu32: A Java-based Tensor Computing Framework with its High-Performance CUDA Library," [Online]. Available: <https://arxiv.org/abs/2305.08819>.
- [16] D. E. Rumelhart, G. E. Hinton and R. Williams, "Learning Representations by Back-Propagating errors," *Nature*, vol. 323, no. 6088, pp. 533-536, Oct. 1986, doi: 10.1038/323533a0.
- [17] L. Orosa, S. Koppula, Y. Umuroglu, K. Kanellopoulos, J. Gomez-Luna, M. Blott, *et al.*, "EcoFlow: Efficient Convolutional Dataflows for Low-Power Neural Network Accelerators," arXiv e-prints, Feb. 2022.
- [18] J. Chang, K. Kang and S. Kang, "An Energy-Efficient FPGA-Based Deconvolutional Neural Networks Accelerator for Single Image Super-Resolution," in *IEEE Transactions on Circuits and Systems for Video Technology*, vol. 30, no. 1, pp. 281-295, Jan. 2020, doi: 10.1109/TCSVT.2018.2888898.
- [19] K. Chang and T. Chang, "Efficient Accelerator for Dilated and Transposed Convolution with Decomposition," *IEEE ISCAS*, Seville, Spain, 2020, pp. 1-5, doi: 10.1109/ISCAS45731.2020.9180402.
- [20] A. M. Vadakkevedu, D. Mandal, P. Ramachandran and N. Chandrachoodan, "Split-Knit Convolution: Enabling Dense Evaluation of Transpose and Dilated Convolutions on GPUs," *IEEE 29th HiPC*, Bengaluru, India, 2022, pp. 1-10, doi: 10.1109/HiPC56025.2022.00014.
- [21] Zhiyi Zhang, "Dragon-Alpha." [Online]. Available: <https://github.com/GilgameshXYZ123/Dragon-Alpha>.
- [22] NVIDIA, "CUDA C Programming Guide," [Online]. Available: <https://docs.nvidia.com/cuda/cuda-c-programming-guide>.
- [23] NVIDIA, "CUDA C Best Practices Guide," [Online]. Available: <https://docs.nvidia.com/cuda/cuda-c-best-practices-guide>.
- [24] NVIDIA, "NVIDIA Turing GPU Architecture," [Online]. Available: <https://images.nvidia.com/aem-dam/en-zz/Solutions/design-visualization/technologies/turing-architecture/NVIDIA-Turing-Architecture-Whitepaper.pdf>.
- [25] A. Krizhevsky, "Cifar10," [Online]. Available: <http://www.cs.toronto.edu/~kriz/cifar.html>.

APPENDIX

Algorithm. 1 <i>ConvV2</i>	Algorithm. 2 <i>KS-deconv:Stage1</i>
Input: input-features $\mathbf{X} \in \mathbf{R}^{N \times I_H \times I_W \times I_C}$, filters $\mathbf{W} \in \mathbf{R}^{O_C \times F_H \times F_W \times I_C}$, stride $\langle sh \ sw \rangle$, padding $\langle ph \ pw \rangle$ Output: output-features $\mathbf{Y} \in \mathbf{R}^{N \times O_H \times O_W \times O_C}$ for $\mathbf{Y}_{n, oh, ow, oc}$ in \mathbf{Y} $\langle ih_s \ iw_s \rangle = \langle oh, ow \rangle \odot \langle sh \ sw \rangle - \langle ph \ pw \rangle$ $\langle fh_s \ fh_e \rangle = \langle \max(-ih_s, 0) \min(I_H - ih_s, F_H) \rangle$ $\langle fw_s \ fw_e \rangle = \langle \max(-iw_s, 0) \min(I_W - iw_s, F_W) \rangle$ $\mathbf{Y}_{n, oh, ow, oc} = \sum_{\substack{fh \in [fh_s, fh_e] \\ fw \in [fw_s, fw_e] \\ ic \in \{0, I_C\}}} \mathbf{X}_{n, (ih_s+fh), (iw_s+fw), ic} * \mathbf{W}_{oc, fh, fw, ic}$	Input: filters $\mathbf{W} \in \mathbf{R}^{O_C \times F_H \times F_W \times I_C}$, stride $\langle sh \ sw \rangle$ Output: the smaller kernels $\mathbf{C} \in \mathbf{R}^{sh \times sw \times O_C \times \lfloor \frac{F_H}{sh} \rfloor \times \lfloor \frac{F_W}{sw} \rfloor \times I_C}$ Initialize: $\mathbf{C} = \mathbf{0}$ for $\mathbf{C}_{y, x}$ in \mathbf{C} $\langle oph_{y, x} \ opw_{y, x} \rangle = \langle \lfloor \frac{F_H - y}{sh} \rfloor \lfloor \frac{F_W - x}{sw} \rfloor \rangle - \vec{1}$ for $\mathbf{C}_{y, x, oc, ch, cw}$ in $\mathbf{C}_{y, x}$ $\langle fh \ fw \rangle = \langle y \ x \rangle + \langle oph_{y, x} - ch \ opw_{y, x} - cw \rangle \odot \langle sh \ sw \rangle$ $\mathbf{C}_{y, x, oc, ch, cw} = \mathbf{W}_{oc, fh, fw}$ if $\langle fh \ fw \rangle$ in-range-of \mathbf{W}

Algorithm. 2 <i>KS-deconv:Stage2&3</i>	Algorithm. 2B <i>KS-deconv-V2:Stage2&3</i>
<p>Input: gradient of output-features $\nabla Y \in \mathbf{R}^{N \times O_H \times O_W \times O_C}$, the smaller kernels $\mathbf{C} = \mathbf{0} \in \mathbf{R}^{sh \times sw \times O_C \times \left\lfloor \frac{F_H}{sh} \right\rfloor \times \left\lfloor \frac{F_W}{sw} \right\rfloor \times I_C}$, stride $\langle sh \ sw \rangle$, padding $\langle ph \ pw \rangle$</p> <p>Output: gradient of input-features $\nabla X \in \mathbf{R}^{N \times I_H \times I_W \times I_C}$</p> <p>for $\mathbf{C}_{y,x}$ in \mathbf{C}</p> <p>$\langle ih_s \ iw_s \rangle = \langle y \ x \rangle - \langle ph \ pw \rangle$</p> <p>$\langle ih_s \ iw_s \rangle += \langle 1_{ih_s < 0} \ 1_{iw_s < 0} \rangle \odot \left\langle \left\lfloor \frac{-ih_s}{sh} \right\rfloor \left\lfloor \frac{-iw_s}{sw} \right\rfloor \right\rangle \odot \langle sh \ sw \rangle$</p> <p>for $\langle n \ u \ v \ ic \rangle = \vec{0}$ to $\langle N \ \left\lfloor \frac{I_H}{sh} \right\rfloor \left\lfloor \frac{I_W}{sw} \right\rfloor I_C \rangle - \vec{1}$</p> <p>$\langle ih \ iw \rangle = \langle u \ v \rangle \odot \langle sh \ sw \rangle + \langle ih_s \ iw_s \rangle$</p> <p>$\langle oh_s \ ow_s \rangle = \left\langle \left\lfloor \frac{ih+ph-y}{sh} \right\rfloor \left\lfloor \frac{iw+pw-x}{sw} \right\rfloor \right\rangle - \langle oph_{y,x} \ opw_{y,x} \rangle$</p> <p>continue if $\langle ih \ iw \rangle$ not in-range-of ∇X</p> <p>$\nabla X_{n,ih,ic} = 0$</p> <p>for $\mathbf{C}_{y,x,oc,chw,ic}$ in $\mathbf{C}_{y,x}$:</p> <p>$\langle oh \ ow \rangle = \langle oh_s \ ow_s \rangle + \langle ch \ cw \rangle$</p> <p>continue if $\langle oh \ ow \rangle$ not in-range-of ∇Y</p> <p>$\nabla X_{n,ih,ic} += \nabla Y_{n,oh,ow,oc} * \mathbf{C}_{y,x,oc,chw,ic}$</p>	<p>Input: gradient of output-features $\nabla Y \in \mathbf{R}^{N \times O_H \times O_W \times O_C}$, the smaller kernels $\mathbf{C} = \mathbf{0} \in \mathbf{R}^{sh \times sw \times O_C \times \left\lfloor \frac{F_H}{sh} \right\rfloor \times \left\lfloor \frac{F_W}{sw} \right\rfloor \times I_C}$, stride $\langle sh \ sw \rangle$, padding $\langle ph \ pw \rangle$</p> <p>Output: gradient of input-features $\nabla X \in \mathbf{R}^{N \times I_H \times I_W \times I_C}$</p> <p>for $\mathbf{C}_{y,x}$ in \mathbf{C}</p> <p>$\langle \mathbf{C}_H^{y,x} \ \mathbf{C}_W^{y,x} \rangle = \left\langle \left\lfloor \frac{F_H-y}{sh} \right\rfloor \left\lfloor \frac{F_W-x}{sw} \right\rfloor \right\rangle$</p> <p>$\langle ih_s \ iw_s \rangle = \langle y \ x \rangle - \langle ph \ pw \rangle$</p> <p>$\langle ih_s \ iw_s \rangle += \langle 1_{ih_s < 0} \ 1_{iw_s < 0} \rangle \odot \left\langle \left\lfloor \frac{-ih_s}{sh} \right\rfloor \left\lfloor \frac{-iw_s}{sw} \right\rfloor \right\rangle \odot \langle sh \ sw \rangle$</p> <p>for $\langle n \ u \ v \ ic \rangle = \vec{0}$ to $\langle N \ \left\lfloor \frac{I_H}{sh} \right\rfloor \left\lfloor \frac{I_W}{sw} \right\rfloor I_C \rangle - \vec{1}$</p> <p>$\langle ih \ iw \rangle = \langle u \ v \rangle \odot \langle sh \ sw \rangle + \langle ih_s \ iw_s \rangle$</p> <p>$\langle oh_s \ ow_s \rangle = \left\langle \left\lfloor \frac{ih+ph-y}{sh} \right\rfloor \left\lfloor \frac{iw+pw-x}{sw} \right\rfloor \right\rangle - \langle oph_{y,x} \ opw_{y,x} \rangle$</p> <p>$\langle ch_s \ ch_e \rangle = \left\langle \max(-oh_s, 0) \min(O_H - oh_s, oph_{y,x}) \right\rangle$</p> <p>$\langle cw_s \ cw_e \rangle = \left\langle \max(-ow_s, 0) \min(O_W - ow_s, opw_{y,x}) \right\rangle$</p> <p>continue if $\langle ih \ iw \rangle$ not in-range-of ∇X</p> <p>$\nabla X_{n,ih,ic} = \sum_{\substack{ch \in [ch_s, ch_e] \\ cw \in [cw_s, cw_e] \\ ic \in [0, I_C]}} \nabla Y_{n,(oh_s+ch),(ow_s+cw),oc} * \mathbf{C}_{y,x,oc,chw,ic}$</p>

Algorithm. 3 <i>Sk-dilated</i>	Algorithm. 3B <i>Sk-dilated-V2</i>
<p>Input: gradient of output-features $\nabla Y \in \mathbf{R}^{N \times OH \times OW \times OC}$, input-features $\mathbf{X} \in \mathbf{R}^{N \times IH \times IW \times IC}$, stride $\langle sh \ sw \rangle$, padding $\langle ph \ pw \rangle$</p> <p>Output: gradient of filters $\nabla W \in \mathbf{R}^{OC \times FH \times FW \times IC}$</p> <p>for $\nabla W_{oc,fh,fw,ic}$ in ∇W</p> <p>$\langle ih_s \ iw_s \rangle \nabla W_{oc,fh,fw,ic} = \langle fh - ph \ fw - pw \ 0 \rangle$</p> <p>for $\nabla Y_{n,oh,ow,oc}$ in ∇Y</p> <p>$\langle ih \ iw \rangle = \langle oh, ow \rangle \odot \langle sh \ sw \rangle + \langle ih_s \ iw_s \rangle$</p> <p>continue if $\langle ih \ iw \rangle$ not in-range-of \mathbf{X}</p> <p>$\nabla W_{oc,fh,fw,ic} += \mathbf{X}_{n,ih,ic} * \nabla Y_{n,oh,ow,oc}$</p>	<p>Input: gradient of output-features $\nabla Y \in \mathbf{R}^{N \times OH \times OW \times OC}$, input-features $\mathbf{X} \in \mathbf{R}^{N \times IH \times IW \times IC}$, stride $\langle sh \ sw \rangle$, padding $\langle ph \ pw \rangle$</p> <p>Output: gradient of filters $\nabla W \in \mathbf{R}^{OC \times FH \times FW \times IC}$</p> <p>for $\nabla W_{oc,fh,fw,ic}$ in ∇W</p> <p>$\langle ih_s \ iw_s \rangle = \langle fh - ph \ fw - pw \rangle$</p> <p>$\langle oh_s \ oh_e \rangle = \left\langle \max\left(\left\lfloor \frac{-ih_s}{sh} \right\rfloor, 0\right) \min\left(O_H, \left\lfloor \frac{I_H-ih_s}{sh} \right\rfloor\right) \right\rangle$</p> <p>$\langle ow_s \ ow_e \rangle = \left\langle \max\left(\left\lfloor \frac{-iw_s}{sw} \right\rfloor, 0\right) \min\left(O_W, \left\lfloor \frac{I_W-iw_s}{sw} \right\rfloor\right) \right\rangle$</p> <p>$\nabla W_{oc,fh,fw,ic} = \sum_{\substack{oh \in [oh_s, oh_e] \\ ow \in [ow_s, ow_e] \\ n \in [0, N]}} \mathbf{X}_{n,(ih_s+oh*sh),(iw_s+ow*sw),ic} * \nabla Y_{n,oh,ow,oc}$</p>